12 **pyisotopomer: A Python package for obtaining nitrous oxide isotopocules from isotope**
13 **ratio mass spectrometry**

Colette L. Kelly,[1*] Cara Manning,[2] Claudia Frey,[3] Noah Gluschankoff,[1] and Karen L. Casciotti

14

15 1. Stanford University, Department of Earth System Science, Stanford, CA 94305, USA
16 2. University of Connecticut, Department of Marine Sciences, Groton, CT, 06340, USA
17 3. Department of Environmental Science, University of Basel, Basel, Switzerland.
18
19 *** Correspondence to:** Colette L. Kelly (email: clkelly@stanford.edu; address: 473 Via Ortega
20 Room 140, Stanford, CA 94305).

21
22 **Keywords:** Nitrous oxide, isotopomers, nitrogen stable isotopes, scrambling, Python
23

24 **Abstract**

25

26 **RATIONALE** Obtaining nitrous oxide isotopocule measurements with isotope ratio mass
27 spectrometry (IRMS) requires measuring the m/z ratios of the nitrous oxide (N_2O) molecule as
28 well as those of the NO^+ fragment ion. This measurement depends on correcting for a
29 phenomenon referred to as "scrambling" in the ion source, whereby the NO^+ fragment ion
30 contains the outer N atom from the N_2O molecule. While descriptions of the scrambling
31 correction exist in the literature, there has yet to be published a unified software package and
32 method for performing this correction.

33

34 **METHODS** We developed a user-friendly Python package (pyisotopomer), with a MATLAB
35 alternative, to determine two coefficients that describe scrambling in the ion source of a given
36 IRMS, and then to use this calibration to obtain N_2O isotopocule measurements.

37

38 **RESULTS** We assess the sensitivity of pyisotopomer to its input parameters and discuss the
39 relevant assumptions. We show that the scrambling behavior of an IRMS can vary with time,
40 necessitating regular calibrations. We show that to obtain a relative uncertainty in site preference
41 of <1‰, the relative uncertainty in each scrambling coefficient should be <0.2%. Finally, we
42 present an intercalibration between two IRMS laboratories, using pyisotopomer to calculate
43 scrambling and obtain N_2O isotopocule data.

44

45 **CONCLUSIONS** Given these considerations, we discuss how to use this software package to
46 obtain high-quality N_2O isotopocule data from IRMS systems, including the use of appropriate
47 reference materials and frequency of calibration.

1. Introduction

Nitrous oxide (N_2O) is a potent greenhouse gas, with a greenhouse gas potential approximately 265 times that of carbon dioxide, over 100 years and on a per-molecule basis.[1,2] N_2O is also likely to be the most important ozone depletion agent of the 21st century, due to production of NO radicals in the stratosphere that interact destructively with ozone.[3–6] Historically, the bulk stable isotopes of nitrogen and oxygen in N_2O have been used to quantify its microbial cycling in soils,[7,8] its destruction by photolysis and cycling in the atmosphere,[9,10] and microbial cycling in the ocean.[11–14] This approach often does not provide a unique solution, because the bulk nitrogen and oxygen isotope ratios of N_2O depend on the isotopic composition of the substrate, as well as the isotope effects of production and consumption processes.[14] Furthermore, in the context of microbial N_2O cycling in soils and the ocean, bacterial nitrification and denitrification produce N_2O with similar bulk $\delta^{15}N$ values, which prevents partitioning between these processes on the basis of bulk $\delta^{15}N$ alone.[15,16] This leaves room for a more nuanced measurement, which may distinguish between N_2O production processes in the soils, atmosphere, and ocean.

Given the asymmetry of the N_2O molecule, its two nitrogen atoms exist in unique chemical environments, making the molecule particularly rich in isotopic information. The individual isotopic compositions of each nitrogen atom were first measured by Friedman and Bigeleisen, who quantified the yields of isotopomers $^{14}N^{15}N^{16}O$ and $^{15}N^{14}N^{16}O$ from enriched ammonium nitrate by measuring the ion beam signal of the fragment ion NO^+ in an isotope ratio mass spectrometer.[17] The natural abundance isotopomers of N_2O were quantified 50 years later with a similar technique, by measuring the molecular N_2O mass to charge (m/z) ratios 44, 45, and 46 as well as the m/z ratios 30 and 31 of the NO^+ fragment ion.[18,19] Toyoda and Yoshida (1999) defined the site-specific isotope ratios of the central (α) nitrogen atom and outer (β) nitrogen atom as follows:

$$^{15}R^\alpha = \frac{^{14}N^{15}NO}{^{14}N^{14}NO} \tag{1}$$

$$^{15}R^\beta = \frac{^{15}N^{14}NO}{^{14}N^{14}NO} \tag{2}$$

The N_2O isotopomer measurement was initially performed with two sequential measurements of the same sample on an isotope ratio mass spectrometer, one for m/z ratios 44, 45, and 46, and one for m/z ratios 30 and 31.[18] Subsequent advances led to the measurement of all five m/z ratios simultaneously with the correct configuration of cups.[20]

The slight difference in zero-point energies between the isotopomers of N_2O result in different isotopic fractionations during photolysis in the stratosphere,[21] making the isotopomers of N_2O a powerful tool for understanding its atmospheric cycling.[22–26] Likewise, N_2O site preference, defined as $\delta^{15}N^\alpha - \delta^{15}N^\beta$, was shown in microbial culture experiments to be largely a function of reaction mechanism, independent of source composition.[27–32] This allowed for the differentiation between N_2O deriving from bacterial nitrification and denitrification, although some debate exists about whether the site preference of N_2O produced by denitrifying bacteria is closer to 0‰ or 25‰,[31,33] the latter possibility being largely ignored in subsequent literature. During N_2O consumption, $\delta^{15}N^\alpha$ and $\delta^{18}O_{N2O}$ were shown in microbial culture[34] and soil mesocosm[35] experiments to exhibit a characteristic relationship, allowing subsequent studies to

89　use this expected relationship to distinguish between oxidative and reductive regimes of N_2O
90　cycling.[36,37]
91　　　The site-specific isotopomers of N_2O provide a far more nuanced constraint on the
92　biogeochemical cycling of N_2O than its bulk composition alone. N_2O isotopomers have been
93　used extensively to quantify its biogeochemical cycling in soils[35,38–40] the atmosphere,[22,29] and
94　the ocean.[27,36,37,41–48] Nonetheless, there is as yet no unified method for calibrating isotope ratio
95　mass spectrometry systems for the N_2O isotopomer (and isotopocule) measurement. The need for
96　such a calibration is largely due to a phenomenon called "scrambling," whereby the NO^+
97　fragment ion contains the outer, β nitrogen atom, rather than the expected α nitrogen. A number
98　of approaches have been taken to calibrate an IRMS system for this effect: the use of a single
99　"rearrangement factor" to describe scrambling,[18,49] the use of nine coefficients to describe the
100　different fragmentation behaviors of the different isotopocules of N_2O,[50] and finally the use of
101　two coefficients to describe scrambling in the ion source.[32] While descriptions exist of each of
102　these approaches, and international intercalibration efforts have been made,[51,52] there has yet to
103　be published a package of code for implementing one of the above isotopomer calibrations.
104　　　We developed a Python software package that implements the two-coefficient approach
105　described by Frame and Casciotti (2010) to calibrate an IRMS system for scrambling and use
106　that calibration to obtain high-quality N_2O isotopocule data. To quantify the performance of the
107　software, we tested its sensitivity to solver parameters and the assumptions inherent to the
108　scrambling equations. Next, we quantified the uncertainty associated with different pairings of
109　reference materials used to calculate scrambling and compared the outputs from the MATLAB
110　and Python versions of the software. To quantify the variability of the fragmentation behavior of
111　an instrument over time, we examined the scrambling coefficients for one isotope ratio mass
112　spectrometer over the course of four years of measurements. To assess the effect of uncertainty
113　in each scrambling coefficient on calculated isotopocule values, we used a Monte Carlo
114　simulation approach to quantify the effect of uncertainty in the scrambling coefficients on the
115　final, output N_2O isotopocule values. Finally, we performed an intercalibration using this
116　software across two labs at Stanford and the University of Basel.
117
118　**2. Theory**
119　　　Toyoda and Yoshida (1999) introduced the isotopomer notation in equations 1 and 2,
120　designating the inner and outer nitrogen atoms as the α and β nitrogen atoms, respectively. The
121　expressions for molecular m/z ratios 45/44 (^{45}R) and 46/44 (^{46}R), used for two different
122　calibration approaches,[18,49] follow from this notation:
123

$$^{45}R = {}^{15}R^{\alpha} + {}^{15}R^{\beta} + {}^{17}R \tag{3}$$

$$^{46}R = ({}^{15}R^{\alpha} + {}^{15}R^{\beta}){}^{17}R + {}^{18}R + ({}^{15}R^{\alpha})({}^{15}R^{\beta}) \tag{4}$$

124　where $^{15}R^{\alpha}$ denotes the isotopocule ratio $^{14}N^{15}N^{16}O/^{14}N^{14}N^{16}O$, $^{15}R^{\beta}$ denotes the isotopocule ratio
125　$^{15}N^{14}N^{16}O/^{14}N^{14}N^{16}O$, ^{17}R denotes the isotopocule ratio $^{14}N^{14}N^{17}O/^{14}N^{14}N^{16}O$, and ^{18}R denotes
126　the isotopocule ratio $^{14}N^{14}N^{18}O/^{14}N^{14}N^{16}O$.
127　　　While the oxygen triple isotopes of N_2O ($\Delta^{17}O$) provide additional information about the
128　sources and sinks of N_2O,[53,54] they will not be discussed further here. Thus, we will assume that
129　^{17}R covaries with ^{18}R according to the oxygen isotope content of Vienna Standard Mean Ocean
130　Water (VSMOW)[55,56] and a mass-dependent relationship between ^{17}R and ^{18}R:[53]

131
$$^{17}R/0.0003799 = (^{18}R/0.0020052)^{0.516} \tag{5}$$

132   The simplest formulation for the NO$^+$ fragment ion ratio 31/30 (^{31}R) comes from Toyoda
133 and Yoshida (1999):

$$^{31}R = {}^{15}R^\alpha + {}^{17}R \tag{6}$$

134   This equation would represent the ^{31}R measured by IRMS if no scrambling occurred.
135 Indeed, given a known $^{15}R^\alpha$ and ^{17}R for a reference gas, this equation defines the theoretical ^{31}R
136 of that reference gas. Toyoda and Yoshida (1999) account for scrambling by defining the
137 rearrangement factor y (which was later redefined as γ) as "the fraction of NO$^+$ bearing the β
138 nitrogen of the initial N$_2$O to the total NO$^+$ formed," to yield:
139

$$^{31}R = (1-\gamma)^{15}R^\alpha + \gamma^{15}R^\beta + {}^{17}R \tag{7}$$

140   Kaiser et al. (2004) introduce a more complete representation of ^{31}R, adding terms for
141 ^{15}N^{15}N^{16}O, ^{14}N^{15}N^{17}O, and ^{15}N^{14}N^{17}O to m/z=31, and terms for ^{15}N^{14}N^{16}O and ^{14}N^{15}N^{16}O to
142 m/z=30:
143

$$^{31}R = \frac{(1-\gamma)^{15}R^\alpha + \gamma^{15}R^\beta + (^{15}R^\alpha)(^{15}R^\beta) + {}^{17}R(1 + \gamma^{15}R^\alpha + (1-\gamma)^{15}R^\beta)}{1 + \gamma^{15}R^\alpha + (1-\gamma)^{15}R^\beta} \tag{8}$$

144   Note that Kaiser et al. (2004), in their Eqn. (3), use the term "s" in place of γ, $^{15}R_{1,\text{ref}}$ in
145 place of $^{15}R^\beta$, and $^{15}R_{2,\text{ref}}$ in place of $^{15}R^\alpha$. To account for different fragmentation rates from
146 different isotopic species of N$_2$O, Westley et al. (2007) split the fragmentation factor γ into nine
147 coefficients:
148

$$^{31}R = \frac{a_{31}{}^{15}R^\alpha + b_{31}{}^{15}R^\beta + c_{31}(^{15}R^\alpha)(^{15}R^\beta) + {}^{17}R(d_{31} + e_{31}{}^{15}R^\alpha + f_{31}{}^{15}R^\beta)}{1 + a_{30}{}^{15}R^\alpha + b_{30}{}^{15}R^\beta + c_{30}(^{15}R^\alpha)(^{15}R^\beta)} \tag{9}$$

149   While this approach considers the possibility of different rates of fragmentation for every
150 isotopic species of N$_2$O (i.e., isotopic fractionation) measurable with this IRMS configuration, it
151 also requires solving for six to nine coefficients, depending on whether the m/z=30 coefficients
152 are considered separate from the m/z=31 coefficients. Frame and Casciotti (2010) simplify this
153 equation by reducing the number of fragmentation factors to two coefficients, γ and κ, which
154 represent the yield of ^{30}NO$^+$ from ^{14}N^{15}NO (for both ^{17}O and ^{16}O) and the yield of ^{31}NO$^+$ from
155 ^{15}N^{14}NO, respectively. This yields the equation:
156

$$^{31}R = \frac{(1-\gamma)^{15}R^\alpha + \kappa^{15}R^\beta + (^{15}R^\alpha)(^{15}R^\beta) + {}^{17}R(1 + \gamma^{15}R^\alpha + (1-\kappa)^{15}R^\beta)}{1 + \gamma^{15}R^\alpha + (1-\kappa)^{15}R^\beta} \tag{10}$$

157   The important pieces of information contained within the two scrambling factors are the
158 unequal rates of fragmentation for the isotopomers ^{14}N^{15}NO and ^{15}N^{14}NO, which the equation
159 from Kaiser et al. (2004) does not account for. It is assumed that the isotopic substitution of ^{17}O
160 in the oxygen atom has a negligible effect on the scrambling coefficients, or, in terms of the

161 equation from Westley et al. (2007), that $e_{31}=(1-a_{31})$ and $f_{31}=(1-b_{31})$. It is also assumed that the
162 coefficient c_{31} from Westley et al. (2007) is equal to 1, or that the yield of $^{31}NO^+$ from $^{15}N^{15}N^{16}O$
163 is equal to the yield of $^{30}NO^+$ from $^{14}N^{14}N^{16}O$. Given that naturally occurring N_2O contains very
164 little of the $^{15}N^{15}N^{16}O$ isotopocule, a few per mil difference in the fractionation during
165 fragmentation of $^{15}N^{15}N^{16}O$ and $^{14}N^{14}N^{16}O$ would not drastically alter the measured ^{31}R.[57]
166 Finally, the coefficient d_{31} is assumed to be equal to 1, or that the yield of $^{31}NO^+$ from $^{14}N^{14}N^{17}O$
167 is equal to the yield of $^{30}NO^+$ from $^{14}N^{14}N^{16}O$, again, an assumption yielding little potential error
168 in ^{31}R, given the low natural abundance of ^{17}O in N_2O.[53]
169   Measurement of two reference materials against a common third reference gas, each with
170 known $^{15}R^{\alpha}$ and $^{15}R^{\beta}$ values, produces two equations to solve for two unknowns, γ and κ,
171

$$\frac{^{31}R_{sample1}}{^{31}R_{reference}} - \frac{[rR31/30_{sample1}]}{[rR31/30_{reference}]} = 0 \tag{11}$$

172

$$\frac{^{31}R_{sample2}}{^{31}R_{reference}} - \frac{[rR31/30_{sample2}]}{[rR31/30_{reference}]} = 0 \tag{12}$$

173

174   Where $^{31}R_{sample1}$ is the theoretical ^{31}R of the first reference material, calculated from
175 equation 10, $^{31}R_{reference}$ is the theoretical ^{31}R of the common reference gas against which sample
176 peaks are normalized, and $^{31}R_{sample2}$ is the theoretical ^{31}R of the second reference material. These
177 "ratios of ratios" should be equivalent to the measured ^{31}R of each reference material normalized
178 to the common reference injection, leaving a set of cost functions to be minimized. To aid in
179 finding a solution, equations 11 and 12 may be simplified by assuming that the ^{31}R of the direct
180 reference injection is constant ("C", below), and thus that the flat-topped reference peak has a
181 defined scrambling behavior that could differ from that of a sample peak. Calculating 'C' for the
182 common reference injection from equation 10, using assumed γ and κ values, produces the
183 following two equations:

$$\frac{^{31}R_{sample1}}{C} - \frac{[rR31/30_{sample1}]}{[rR31/30_{reference}]} = 0 \tag{13}$$

184

$$\frac{^{31}R_{sample2}}{C} - \frac{[rR31/30_{sample2}]}{[rR31/30_{reference}]} = 0 \tag{14}$$

185

186   Given a pair of reference materials with known $^{15}R^{\alpha}$ and $^{15}R^{\beta}$, pyisotopomer[58] solves
187 equations 13 and 14 for scrambling coefficients γ and κ. Pyisotopomer uses the "least_squares"
188 function from the scipy optimization library to vary γ and κ until the calculated values of
189 $^{31}R_{sample}/^{31}R_{reference}$ are as close to $[rR31NO/30NO_{sample}/R31NO/30NO_{reference}]$, as described in
190 Frame and Casciotti (2010). In MATLAB, the solver lsqnonlin is used to perform the
191 optimization.
192   After the scrambling coefficients are calculated from measured reference materials,
193 pyisotopomer can be used to calculate the $^{15}R^{\alpha}$ and $^{15}R^{\beta}$ of unknown samples using equations 3,
194 4, and 10. These equations are solved for the $^{15}R^{\alpha}$ and $^{15}R^{\beta}$, from measured isotope ratios ^{31}R,
195 ^{45}R, and ^{46}R of the unknown. As in the scrambling function, pyisotopomer uses least_squares
196 from scipy.optimize to solve this set of equations, producing the isotope ratios $^{15}R^{\alpha}$, $^{15}R^{\beta}$, ^{17}R,

197 and ^{18}R, and from these, the delta values $\delta^{15}N^\alpha$, $\delta^{15}N^\beta$, site preference, $\delta^{15}N^{bulk}$, $\delta^{17}O_{N2O}$, and
198 $\delta^{18}O_{N2O}$ are calculated relative to primary reference scales (^{15}R from atmospheric N_2 and ^{17}R and
199 ^{18}R from VSMOW).
200
201 **3. Experimental**
202 **3.1 Preparation and analysis of N$_2$O reference materials**
203   To validate the usage of pyisotopomer to calculate scrambling coefficients, and from
204 these coefficients obtain precise N$_2$O isotopocule data, a series of N$_2$O reference materials (Table
205 1) were prepared and analyzed in sample format at Stanford University ("Lab 1") and the
206 University of Basel ("Lab 2"). Reference materials were prepared by filling 160-mL glass serum
207 bottles (Wheaton) with de-ionized water and removing a 4-mL headspace (Lab 1) or 10-20-mL
208 headspace (Lab 2), then were capped with a gray butyl septum (National Scientific) and sealed
209 with an aluminum crimp seal. These bottles were purged with helium for 90 minutes to remove
210 all background N$_2$O. The purged bottles were then injected with reference gas in a range of nmol
211 amounts from 2-20 nmols N$_2$O (S2, EMPA1, EMPA2, EMPA3 reference gases) or with 10
212 nmols N$_2$O (B6 reference gas) using a gas-tight syringe. Reference materials prepared in Lab 1
213 were preserved with 100 µL saturated mercuric chloride solution; those prepared in Lab 2
214 contained no added preservative. For Lab 1, atmosphere-equilibrated seawater was prepared by
215 filtering surface seawater (collected in Half Moon Bay, CA) through a 0.22 mm Sterivex filter,
216 allowing it to undergo static equilibration with outdoor air for three days, then re-filtering into
217 160-mL serum bottles, removing a ~1-mL headspace, and preserving with 100 µL saturated
218 mercuric chloride solution. For Lab 2, atmosphere-equilibrated reference materials were
219 prepared by purging either de-ionized water or a sodium chloride solution with helium, allowing
220 it to undergo static equilibration with outdoor air for three days, filling into 160-mL serum
221 bottles, and removing a 10-mL headspace. Reference materials were run in the same format as
222 samples to account for any potential fractionation associated with the extraction and purification
223 of N$_2$O associated with the purge-and-trap system. The magnitude of such fractionation was
224 quantified for Lab 1 by running the pure N$_2$O reference tank against itself, and yielded offsets of
225 0.22±0.52‰ for $\delta^{15}N^{bulk}$ and 0.16±0.62‰ for $\delta^{18}O_{N2O}$.
226   The isotopocule values for each reference gas were calibrated independently by J. Mohn
227 (EMPA; mini-QCLAS aerodyne) or S. Toyoda (Tokyo Tech; IRMS), except for one internal
228 standard used by Lab 1 (Table 1). The reported ^{31}R, ^{45}R, and ^{46}R for the pure N$_2$O reference
229 tanks represent the theoretical values of these ratios, assuming some amount of scrambling for
230 the reference gas: $\gamma=0.17$ and $\kappa=0.08$ (Stanford University/Lab 1), and $\gamma=0.156$ and $\kappa=0.155$
231 (University of Basel/Lab 2). The values for $\delta^{17}O_{N2O}$ for each gas were calculated assuming a
232 mass-dependent relationship between ^{17}R and ^{18}R.[53]
233   These reference gases and samples were measured on Thermo Finnigan DELTA V^{PLUS}
234 isotope ratio mass spectrometers (IRMS; Thermo Fisher Scientific, Waltham, MA) in Lab 1 and
235 Lab 2. Each IRMS had Faraday cups configured to simultaneously measure *m/z* 30, 31, 44, 45,
236 and 46. Reference materials and samples were analyzed on a custom purge-and-trap system
237 coupled to each IRMS, which was run in continuous flow mode[59] (Table 1). The two systems
238 had slight differences in the purge-and-trap system: in Lab 1, liquid from each sample bottle was
239 transferred to a sparging column to extract the dissolved gases; in Lab 2, each sample was
240 extracted by purging directly from the bottle. The effects of these differences are discussed
241 further in Results and Discussion.
242

3.2 Data corrections

To calibrate each IRMS for scrambling, reference materials prepared as above were run side-by-side on the same day. This was repeated over multiple days. From these runs, a scrambling calibration was obtained as follows: first, each sample peak was compared against a direct injection of pure N_2O from a reference tank (Table 1).[60] Next, sample peaks were normalized to a peak area of 20 Volt-seconds (Vs) to correct for the effect of peak size on measured isotope ratios. This normalization was performed with a linearity relation specific to each IRMS and purge-and-trap system.[37] Then, for each day of analysis, pyisotopomer was used to generate all possible pairings of reference materials on that day. Each pairing of reference materials and the associated size-corrected isotope ratios were used as an input to the Scrambling function of pyisotopomer to calculate a pair of γ and κ, the scrambling coefficients introduced in Eqn. (10). From the resulting array of γ and κ values, γ and κ were averaged to obtain a daily mean. These daily means were further combined into a one-week running average to smooth their variability. The one-week running averages of γ and κ for each system were used to obtain N_2O isotopocules for reference materials and unknowns, using the Isotopomers function of pyisotopomer. Finally, a scale decompression (similar to the two-point offset correction suggested by Mohn et al., 2014) was performed for $\delta^{15}N^{\alpha}$, $\delta^{15}N^{\beta}$, $\delta^{17}O_{N2O}$, and $\delta^{18}O_{N2O}$, based on the mean measured values and calibrated values of the reference materials included in each run. The scale-decompressed values of $\delta^{15}N^{bulk}$ and SP were obtained from the scale-decompressed $\delta^{15}N^{\alpha}$ and $\delta^{15}N^{\beta}$.

The data corrections above are described in the README documents associated with pyisotopomer on the Python Package Index. In brief, comparison against the direct N_2O reference injection and normalization to a peak area of 20 Vs can be accomplished with the appropriate IRMS outputs and the pyisotopomer data input template.[58] The import convention for pyisotopomer is:

```
from pyisotopomer import Scrambling, Isotopomers
```

To calculate scrambling, the only function you need is:

```
Scrambling(inputfile="FILENAME.xlsx", ref1="NAME", ref2="NAME", **kwargs)
```

where "FILENAME.xlsx" is the user-designated file name of the data corrections spreadsheet to be used as the inputfile, "ref1" and "ref2" are the reference materials used to perform the scrambling calibration designated with their user-entered "NAME"s, and "**kwargs" refers to optional additional keyword arguments, such as the initial guess for γ and κ (see section 4.1). Once the scrambling coefficients are determined, the only function needed to calculate isotopomers is:

```
279    Isotopomers(inputfile = "FILENAME.xlsx", scrambling = [0.0..., 0.0...], **kwargs)
```

280
281   where "scrambling" refers to the scrambling coefficients used to calculate isotopomers.
282
283   **3.3 Intercalibration**
284   To validate the scrambling calibration, samples of unknown isotopic composition were
285   collected from Lake Lugano, Switzerland in July 2020 and analyzed separately by both Lab 1
286   and Lab 2. The samples were collected at depths of 10 and 90 meters, including six replicate
287   bottles at each depth. Samples were collected into 160-mL glass serum bottles (Wheaton),
288   overflowing each bottle twice, closing bubble-free, and removing liquid to form a 10-mL
289   headspace comprised of air. Based on the Northern hemisphere monthly mean N_2O mixing ratio
290   for July, 2020,[61] when the samples were collected, an atmospheric headspace of this volume
291   would have contained 0.13 nmols N_2O, and resulted in a ~1 nM overestimation of the
292   concentration of N_2O in each sample after equilibration with the headspace during storage. Each
293   sample was capped with a gray butyl septum (National Scientific) and sealed with an aluminum
294   crimp seal. Samples were promptly preserved with 100 µL saturated mercuric chloride solution
295   and stored at lab temperature (20-22°C). Given the trace amount of N_2O in the atmosphere,
296   negligible amount of atmospheric N_2O were added with the 100 µL of mercuric chloride, and
297   with complete flushing of the bottle during analysis, the effect of the headspace and N_2O
298   partitioning between the gas and liquid phases falls within the analytical uncertainty for N_2O
299   concentration and isotopocule measurements.[37] The six replicate bottles at each depth were split
300   into two groups of three replicate bottles to be measured for N_2O isotopocules by Lab 1 and Lab
301   2, respectively. The scrambling calibration and isotopocule calculations for each set of samples
302   were performed in pyisotopomer, as above.
303
304   **4. Results and Discussion**
305   **4.1 Solver parameters**
306   To understand the sensitivity of the Scrambling function of pyisotopomer to the
307   parameters provided to its solver (initial guess, upper bound, lower bound), we performed a
308   series of numerical experiments with said solver. The first of these experiments involved varying
309   the initial guess, x0 (where x0 is a pair of values for γ and κ). Using a range of 50 initial guesses
310   for γ and κ, evenly spaced between $\gamma = \kappa = 0.05$ and $\gamma = \kappa = 0.20$, scrambling was calculated
311   from four reference materials run in December 2020 on the Lab 1 IRMS. These initial guesses
312   for γ and κ were varied in tandem, such that γ and κ were always initialized at the same value.
313   The solver was subsequently used to obtain a range of 50 solutions for γ and κ corresponding to
314   each of the 50 values of x0, holding the lower bounds for the solver constant at $\gamma=0.0$ and $\kappa=0.0$
315   and the upper bounds constant at $\gamma=1.0$ and $\kappa=1.0$. Using the Isotopomers function of
316   pyisotopomer, these 50 solutions for γ and κ were input as scrambling coefficients to obtain a
317   range of 50 values of $\delta^{15}N^\alpha$, $\delta^{15}N^\beta$, and SP for each of the four reference materials (Table 2).
318   The range of x0 values tested produced a similar range of solutions for γ and κ (Figure
319   S1), although their solutions exhibited a nearly constant offset of ~0.09 (γ and κ are unitless
320   since they are proportions, but they can be understood as percentages, whereby a γ value of 0.20
321   can be understood to mean that 20% of $^{14}N^{15}NO$ undergoing fragmentation yields $^{30}NO^+$ instead
322   of $^{31}NO^+$). The solutions for γ and κ increased as x0 increased, such that the initial guess $\gamma=0.05$

323   and κ=0.05 yielded the solution γ=0.138 and κ=0.0454, and the initial guess γ=0.20 and κ=0.20
324   yielded the solution γ=0.272 and κ=0.182 (Figure S1). Despite the wide range of solutions for γ
325   and κ, when used as scrambling coefficients to calculate isotopocule ratios these solutions
326   yielded nearly constant $\delta^{15}N^{\alpha}$, $\delta^{15}N^{\beta}$, and SP values for the four test reference materials (Table
327   2). The standard deviations of $\delta^{15}N^{\alpha}$ and $\delta^{15}N^{\beta}$ were no greater than 0.07‰, and the standard
328   deviation of SP was no greater than 0.13‰ (Table 2). The calculated $\delta^{15}N^{bulk}$ and $\delta^{18}O_{N2O}$ had a
329   standard deviation of 0.0‰ since they are unaffected by scrambling. This indicates that the
330   parameter best constrained by the scrambling calculation is not the absolute value of γ or κ, but
331   rather their relationship to each other, and that it is this relationship that is uniquely determined
332   by each pair of reference materials and IRMS.
333   Additional numerical experiments were conducted to test the sensitivity of the scrambling
334   solver to the upper and lower bounds provided to it. The lower bounds for both γ and κ were
335   varied from γ=0.0 and κ=0.0 to γ=0.08 and κ=0.08, to yield a range of 50 lower bound inputs.
336   For these experiments, the initial guesses for γ and κ were held constant at γ=0.17 and κ=0.08
337   (standard values for Lab 1) across the range of tested lower bound values. Likewise, the upper
338   bounds for γ and κ were held constant at γ=1.0 and κ=1.0 for the lower bound tests. Varying the
339   lower bounds input to the solver resulted in a much smaller range of solutions than varying x0:
340   with the lower bounds set to γ=0.0 and κ=0.0, the solver yielded γ=0.172 and κ=0.0798; with the
341   lower bounds set to γ=0.08 and κ=0.08, the solver yielded γ=0.172 and κ=0.0800. Again, the
342   difference between γ andγ − κ was consistently ~0.09. It should be noted here that the range of
343   lower bounds was smaller than the range of x0 in the analogous experiment above, because the
344   lower bounds for γ and κ cannot, by definition, exceed the lowest value at which either
345   coefficient is initialized — in this case, 0.08. Using the resulting range of solutions for γ and κ to
346   calculate isotopocules for the four test reference materials, we found that the standard deviations
347   of $\delta^{15}N^{\alpha}$ and $\delta^{15}N^{\beta}$ were no greater than 0.0002‰, and the standard deviation of SP was no
348   greater than 0.0004‰ (Table 2).
349   Repeating this procedure to test the sensitivity of the scrambling solver to its upper
350   bounds yielded similar results. Holding x0 constant at γ=0.17 and κ=0.08 and the lower bounds
351   constant at γ=0.0 and κ=0.0, the upper bounds were varied from γ=0.4 and κ=0.4 to γ=1.0 and
352   κ=1.0 across an array of 50 upper bound inputs. The upper bounds γ=0.4 and κ=0.4 yielded the
353   solutions γ=0.171 and κ=0.0795, and the upper bounds γ=1.0 and κ=1.0 yielded the solutions
354   γ=0.172 and κ=0.0798. From these results, it becomes apparent that the solutions for γ and κ
355   relate more closely to the x0 values γ=0.17 and κ=0.08 than they relate to either the lower or
356   upper bounds input to the solver. In this case, the upper bounds are varied from 0.4 to 1.0 to
357   represent a reasonable range of values — unsurprisingly, the edge case wherein the upper bounds
358   are equal or very close to the initial guesses for γ and κ yields solutions for each coefficient that
359   converge at the upper boundary (not shown). Using the resulting range of γ and κ from varying
360   the upper bounds to calculate isotopocules for the four test reference materials, we found that the
361   standard deviations of $\delta^{15}N^{\alpha}$ and $\delta^{15}N^{\beta}$ were no greater than 0.002‰, and the standard deviation
362   of SP was no greater than 0.005‰ (Table 2). The higher standard deviations in this experiment,
363   compared to the lower bounds experiment, can be attributed to the wider range of input values.
364   From this set of experiments, we can provide three recommendations. Firstly, it may be
365   useful to iterate through the scrambling calculation twice if scrambling coefficients have never
366   been obtained for the given system before. The solution from the first iteration may be used as
367   the initial guess for subsequent iterations, such that the initial guesses for γ and κ are as close to

368   their solved values as possible. This can be accomplished with the "initialguess" argument to the
369   Scrambling function of pyisotopomer:

370   Scrambling(inputfile="FILENAME.xlsx", ref1="NAME", ref2="NAME", initialguess=[0.0...,
371   0.0...])

372

373   Secondly, we recommend setting the lower bounds for the scrambling solver to $\gamma=\kappa=0.0$,
374   representing 0% scrambling for $^{14}N^{15}NO$ and $^{15}N^{14}NO$, respectively. Likewise, we recommend
375   setting the upper bounds to $\gamma=\kappa=1.0$, representing 100% scrambling for $^{14}N^{15}NO$ and $^{15}N^{14}NO$,
376   respectively. These are the defaults for pyisotopomer. We recommend these as the bounds to
377   allow the scrambling solver to search for solutions across the widest possible range of plausible
378   solutions (it wouldn't make sense to have negative scrambling coefficients, and neither would it
379   makes sense to have scrambling coefficients greater than 1) and thus to avoid converging at a
380   boundary. Our third and final recommendation is to carefully consider the bounds of $^{15}R^{\alpha}$ and
381     $^{15}R^{\beta}$ provided to the Isotopomers solver. The default upper bounds are $^{15}R^{\alpha}=^{15}R^{\beta}=1.00$, but they
382   can be set to lower ratios such as $^{15}R^{\alpha}=^{15}R^{\beta}=0.005$ in the example below, corresponding to
383     $\delta^{15}N^{\alpha}=\delta^{15}N^{\beta}=360‰$. This is a reasonable ceiling for natural abundance N_2O measurements, but
384   may artificially constrain $^{15}R^{\alpha}$ and $^{15}R^{\beta}$ in ^{15}N-labelled samples. Thus, is important to consider
385   the context and type of sample when changing default arguments.

386   Isotopomers(inputfile = "FILENAME.xlsx", scrambling = [0.0..., 0.0...], lowerbounds=[0.002,
387   0.002], upperbounds=[0.005, 0.005])

388
389
390   **4.2 Reference injection scrambling**
391   To aid in the optimization process, it is assumed that the flat-topped reference peak could
392   have a slightly different γ and κ from the triangular sample peak. Using Eqn. (10), constant
393   values of γ and κ are used to calculate the ^{31}R of the pure N_2O reference gas from its calibrated
394     $\delta^{15}N^{\alpha}$ and $\delta^{15}N^{\beta}$ (Table 1) and $\delta^{17}O$ values. This ^{31}R of the pure N_2O reference gas is used as the
395   "C" parameter in Eqns. (13) and (14) and is assumed to be constant. To test the sensitivity of
396   pyisotopomer to this assumption, the ^{31}R of the pure N_2O reference gas was re-calculated across
397   a range of γ and κ using Eqn. (10), then substituted into the "C" parameter in equations 13 and
398   14. This range of "C" was combined with the measured isotope ratios for one atmosphere-
399   equilibrated seawater and one S2 reference gas run on the Lab 1 IRMS to calculate γ and κ with
400   the Scrambling function of pyisotopomer. Through this sensitivity test, each theoretical γ and κ
401   for the pure N_2O reference gas (C) was paired with a calculated γ and κ for the instrument based
402   on the paired reference materials (Figure 1).
403   The calculated γ and κ varied linearly with the theoretical γ and κ for the direct reference
404   injection (Figure 1). Varying the reference injection γ from 0.17 to 0.18 and holding the
405   reference injection κ constant at 0.080 (white points in Figure 1) resulted in γ ranging from 0.172
406   to 0.181 (Figure 1A) and κ ranging from 0.080 to 0.079 (Figure 1B). Likewise, holding the

407 reference injection γ constant at 0.17 and varying the reference injection κ from 0.080 to 0.070
408 (gray points in Figure 1) also resulted in γ ranging from 0.172 to 0.181 and κ ranging from 0.080
409 to 0.079. Varying the reference injection γ from 0.17 to 0.18 and varying the reference injection
410 κ from 0.080 to 0.070 (black points in Figure 1) resulted in γ ranging from 0.172 to 0.190 and κ
411 ranging from 0.080 to 0.078.
412   Next, the isotopocules for each reference material were calculated from each pairing of
413 theoretical and calculated γ and κ. Despite the variations in the calculated γ and κ shown in
414 Figure 1, the resulting isotopocule ratios varied by less than 0.3‰ (Table 2). The standard
415 deviations of $\delta^{15}N^\alpha$ and $\delta^{15}N^\beta$ were 0.13‰ for both the atmosphere-equilibrated seawater and S2
416 reference materials, and the standard deviation of SP was 0.27‰ for both reference materials
417 (Table 2). This result indicates that the γ and κ solutions output by pyisotopomer compensate
418 implicitly for the γ and κ assumed for the direct reference injection. Thus, we conclude that the
419 assumption of different scrambling for the flat-topped reference peak and triangular sample peak
420 has a small effect on the calculated isotopocules.
421
422 **4.3 Choosing reference material pairings**
423   To understand the effect of different pairings of reference materials on the outcome of the
424 scrambling calibration, γ and κ were calculated from a collection of reference pairings run over
425 two days. On the Lab 1 IRMS, these pairings included the "S2" and "B6" reference materials, as
426 well as atmosphere-equilibrated seawater N_2O (Table 1), the calibrated isotopocule ratios of
427 which fall within the range of values produced in culture[34,62] and nature.[42,46] The mean and
428 standard deviation of γ and κ were calculated from each of three possible pairings of reference
429 materials: atmosphere-equilibrated seawater and S2 (n=8), atmosphere-equilibrated seawater and
430 B6 (n=6), and S2 and B6 (n=6). Reference material isotopocules were then re-calculated with the
431 mean γ and κ from each pairing. Finally, a pooled standard deviation, calculated as the square
432 root of the average of the squared standard deviations,[63] was calculated from the three sets of
433 scrambling coefficients and isotopocule values (Table S1). The same procedure was performed
434 with three sets of N_2O reference materials ("EMPA1", "EMPA2", and "EMPA3") prepared and
435 run on the Lab 2 IRMS. Unlike the reference materials run in Lab 1, however, one of the Lab 2
436 reference materials ("EMPA2") had a $\delta^{15}N^\beta$ value (94.44‰) much higher than what is found in
437 culture[34,62] or nature.[42,46] Again, the mean and standard deviation of γ and κ were calculated from
438 each of three possible pairings: EMPA1 and EMPA2 (n=37), EMPA1 and EMPA3 (n=37), and
439 EMPA2 and EMPA3 (n=34). The greater number of pairings is due to a greater number of
440 reference materials run per day. Pooled standard deviations were then calculated for γ and κ as
441 well as isotopocule values (Table S1).
442   The pooled standard deviations of γ and κ calculated from the Lab 1 reference materials
443 were 0.0007 and 0.0001, respectively, which correspond to relative uncertainties of 0.39% and
444 0.16% (Table S1). T-tests between pairings of reference materials yielded no significant
445 differences in γ and κ. The pooled standard deviations of $\delta^{15}N^\alpha$, $\delta^{15}N^\beta$, and SP were all less than
446 1‰ (Table S1). The pooled standard deviations of γ and κ calculated from the Lab 2 reference
447 materials were larger, corresponding to relative uncertainties of 0.77% and 1.17% in γ and κ,
448 respectively. This was mostly due to the inclusion of the EMPA2 reference gas — calculating
449 scrambling from just the EMPA1 and EMPA3 reference gases, which did not have extreme
450 values, resulted in relative uncertainties in γ and κ of 0.15% and 0.61%, respectively. T-tests
451 between pairings of reference materials yielded significant differences between the scrambling

452 coefficients calculated from pairings including the EMPA2 reference gas and those without. The
453 inclusion of the EMPA2 reference gas resulted in pooled standard deviations of $\delta^{15}N^\alpha$, $\delta^{15}N^\beta$ of
454 greater than 2‰ and a pooled standard deviation of SP greater than 4‰ (Table S1).
455   Based on these results, we suggest that calculated γ and κ have a dependence on the
456 reference materials used to solve for these parameters, the magnitude of which increases with
457 increasingly extreme values of $\delta^{15}N^\alpha$ and $\delta^{15}N^\beta$. Thus, we caution against using reference
458 materials with values that go far beyond bracketing the unknowns to be analyzed to calculate
459 scrambling coefficients. Instead, we recommend calculating γ and κ from reference materials that
460 bracket the range of $\delta^{15}N^\alpha$ and $\delta^{15}N^\beta$ expected for the unknowns. We also recommend that a
461 scale decompression, if applied, brackets the range of unknowns but excludes reference materials
462 such as EMPA2 that lie far outside the expected ranges of $\delta^{15}N^\alpha$ and $\delta^{15}N^\beta$.
463
464 **4.4 MATLAB vs. Python**
465   To compare the performance of the Python and MATLAB versions of pyisotopomer, a
466 week's worth of paired reference materials (atmosphere-equilibrated seawater, S2 reference gas,
467 and B6 reference gas) from December 2020 was processed in both versions of the software. The
468 resulting mean scrambling coefficients were used to re-calculate isotopocules for each reference
469 material. The differences between MATLAB and Python results for γ and κ were both ~0.001,
470 which represents a significant difference (see section 4.6). Using the MATLAB scrambling
471 coefficients in the MATLAB isotopomers solver, and the Python scrambling coefficients in the
472 Python isotopomers solver, the resulting $\delta^{15}N^\alpha$, $\delta^{15}N^\beta$, and $\delta^{18}O_{N2O}$ (and thus site preference,
473 $\delta^{15}N^{bulk}$ and $\delta^{17}O_{N2O}$), showed extremely similar values (Table S1, Figure 2). Results from
474 MATLAB and Python diverged in the second decimal place for $\delta^{15}N^\alpha$ and $\delta^{15}N^\beta$ (Table S1,
475 Figure 2), and differences in the fourth decimal place for $\delta^{18}O_{N2O}$ (not shown). The final output
476 isotopocule values from MATLAB and Python had pooled standard deviations of 0.028‰,
477 0.026‰, and 0.054‰ for $\delta^{15}N^\alpha$, $\delta^{15}N^\beta$, and SP, respectively. Thus, we recommend that if the
478 MATLAB version of pyisotopomer is used to calculate scrambling, the MATLAB version
479 should also be used to calculate isotopocules, and likewise if the Python version of pyisotopomer
480 is used to calculate scrambling, the Python version should also be used to calculate isotopocules.
481
482 **4.5 Variability in fragmentation behavior**
483   To examine the change in the fragmentation behavior of a single IRMS over time, the
484 scrambling coefficients for the Lab 1 IRMS were compiled from 2018-2021 (Figure 3). A
485 running average was calculated using a window size of 20, equivalent to 20 pairs of reference
486 materials. High volatility in γ and κ in March-April 2019 (sample pair numbers 20-40) coincided
487 with a period where the lab temperature was poorly controlled, and thus exhibited strong day-
488 night variation. Before and after this period, the fragmentation behavior of the instrument
489 exhibited smaller variations (Figure 3). The rolling standard deviation of γ and κ (not shown)
490 confirms that the highest standard deviation of a 20-sample window occurred during April 2019,
491 with the rolling standard deviation in γ equal to 0.0018, or a relative uncertainty of 1.03%, and
492 the rolling standard deviation in κ equal to 0.0025, or a relative uncertainty of 3.40%. The
493 standard deviation of γ across the full dataset of scrambling over time was 0.0019, and the
494 standard deviation of κ across the full dataset was 0.0018.
495   There are several reasons why the scrambling behavior of the ion source might change
496 over time. The NO^+ fragment ion can be produced by one of several routes from N_2O^+.[64,65] The

pathways and associated isotope effects for the formation of fragment ions are affected by collision frequency, the distribution of excited states, and the time spent in the ion source, which suggests that ion source conditions such as vapor pressure, ionizing energy, and accelerating voltage may all influence the fragmentation behavior of an IRMS system at a given time.[50,64–67] For these reasons, performing the scrambling calibration only once is not sufficient to obtain high-quality N_2O isotopocule data. Instead, it is important to recalibrate an IRMS system for scrambling on a regular basis since ion source conditions may change with time and can shift abruptly with events such as filament changes. We recommend using a running average of γ and κ over a window of 20 sample pairs, equal to 5 runs of samples with four potential sample pairs per run, rather than calibrating based on day-to-day variation in γ and κ. If there is high volatility in γ and κ, as seen above in March-April 2019, it may be necessary to shorten this window, at the likely expense of accuracy in isotopocule measurements.

4.6 Sensitivity of isotopomers to uncertainty in scrambling coefficients

To quantify the effect of uncertainty in γ and κ on $\delta^{15}N^{\alpha}$, $\delta^{15}N^{\beta}$, and SP, a Monte Carlo simulation was used to introduce random uncertainty in the γ and κ values used to calculate these isotopomers from the measured isotope ratios of three reference materials run on December 7th, 2020. Based on past instrument performance (see section 4.5), we modeled γ as a random number centered around $\gamma=0.1722$ with a standard deviation of 0.00192, which is the cumulative standard deviation of all values of γ for the Lab 1 IRMS from 2018-2021 and corresponds to a relative uncertainty of 1.11%. Likewise, we modeled κ as a random number centered around $\kappa=0.0797$ with a standard deviation of 0.00184, which is the cumulative standard deviation of all values of κ for the Lab 1 IRMS from 2018-2021 and corresponds to a relative uncertainty of 2.31%. We sampled 1,000 pairs of γ and κ from normal distributions with these means and standard deviations, and then used these values of γ and κ to calculate the 1,000 simulated values of $\delta^{15}N^{\alpha}$, $\delta^{15}N^{\beta}$, and SP for the three measured reference materials ("S2", "B6", and atmosphere-equilibrated seawater; Table 1). We determined the resulting uncertainties in each isotopomer by taking a pooled standard deviation across the three reference materials.

This analysis showed that a small relative uncertainty in each scrambling coefficient can lead to per mil-level errors in $\delta^{15}N^{\alpha}$, $\delta^{15}N^{\beta}$, and SP. Specifically, relative uncertainties of 1.11% and 2.31% in γ and κ, respectively, resulted in pooled standard deviations of 3.61‰ in $\delta^{15}N^{\alpha}$ and $\delta^{15}N^{\beta}$ (the pooled standard deviations for $\delta^{15}N^{\alpha}$ and $\delta^{15}N^{\beta}$ were equivalent), and 7.23‰ in SP (Figure 4). Modeling γ and κ with relative uncertainties 0.39% and 0.16%, instead, which were the uncertainties in each parameter based on reference materials run over two days (see section 4.3), led to pooled standard deviations of 0.98‰ in $\delta^{15}N^{\alpha}$, $\delta^{15}N^{\beta}$, and 1.95‰ in SP (Figure S2).

Performing this exercise along a range of modeled uncertainties in γ and κ produced a response curve of the expected standard deviations in each isotopomer for a given level of uncertainty in in γ and κ (Figure S3). Fitting a linear regression through each curve, we obtain equations of form y=mx+b for SP and $\delta^{15}N^{\alpha}$ (the response curves for $\delta^{15}N^{\alpha}$ and $\delta^{15}N^{\beta}$ were identical). Solving for the uncertainty in γ and κ needed to achieve 1‰ pooled standard deviation for SP gives x=0.197%. In other words, to obtain site preference values with an uncertainty of 1‰, the relative uncertainties in γ and κ should be reduced to less than ~0.2%. Averaging scrambling coefficients over a greater number of reference material pairings under the same ion source conditions should reduce their uncertainty; thus, we recommend calculating γ and κ from

542 a ~1-week moving average, instead of daily. Using a one-week moving average of each
543 scrambling coefficient for the intercalibration exercise below (see section 4.7), we found relative
544 uncertainties in γ and κ of 0.4% and 0.2%, respectively — which are close to this target. We do
545 *not* recommend calculating γ and κ from a cumulative average or cumulative moving average
546 that includes longer term changes in ion source conditions, which can affect γ and κ.
547
548 **4.7 Intercalibration**
549   The application of pyisotopomer was tested through an intercalibration including four
550 reference materials and two Lake Lugano samples measured by two IRMS laboratories (Table
551 3). Pyisotopomer was used to perform the scrambling calibration for each laboratory and to
552 obtain isotopocule ratios. Afterwards, a scale decompression was applied, as described in the
553 Methods. The root mean square deviation (RMSD) for each reference material was calculated by
554 comparison to the calibrated values provided by a previous intercalibration effort[52] (atmosphere-
555 equilibrated seawater) and J. Mohn (EMPA1, EMPA2, and EMPA3).
556   The $\delta^{15}N^{bulk}$ measured by the two labs displayed good agreement for three out of the four
557 reference materials, as well as the lake water samples. The $\delta^{15}N^{bulk}$ RMSDs for atmosphere-
558 equilibrated seawater and reference material EMPA3 were 0.71‰ and 0.50‰, respectively, both
559 of which represent an improvement upon the intercalibration presented by Mohn et al. (2014). In
560 contrast, the RMSD for EMPA1 was 2.46‰, larger than the 0.8‰ presented for IRMS labs by
561 Mohn et al., 2014 (Table 3). The RMSD for EMPA2 was highest at 3.59‰, but this is to be
562 expected, given that EMPA2 was excluded from the scrambling calculation and scale
563 decompression conducted in this study due to its extreme values (see section 4.3). For the lake
564 water sample taken at 10 m depth, the $\delta^{15}N^{bulk}$ values measured by Lab 1 and Lab 2 were
565 statistically indistinguishable (Table 3; Figure S4). For the lake water sample taken at 90 m
566 depth, the $\delta^{15}N^{bulk}$ values measured by Lab 1 and Lab 2 were -5.00±0.08‰ and -6.29±1.06‰,
567 respectively (Table 3; Figure S4).
568   The $\delta^{15}N^{\alpha}$ measured by the two labs also showed good agreement for reference materials
569 EMPA1, EMPA3, and atmosphere-equilibrated seawater: in each case, the combined RMSD was
570 less than 2.60‰ (Table 3). This is similar to the data presented in Mohn et al. (2014), who find
571 an RMSD for $\delta^{15}N^{\alpha}$ for IRMS laboratories of 2.47‰. The values of $\delta^{15}N^{\alpha}$ measured by the two
572 labs for the lake water unknowns differed by ~2-3‰, but no consistent offset emerged between
573 the two labs, and neither did such an offset emerge in the reference materials (i.e., the values for
574 some samples were higher in Lab 1, and others are higher for Lab 2; Figure S4). For $\delta^{15}N^{\beta}$, the
575 RMSD for atmosphere-equilibrated seawater, EMPA1, and EMPA3 were slightly larger, and
576 only EMPA3 represents an improvement upon the data presented in previous intercalibrations
577 (Table 3). The $\delta^{15}N^{\beta}$ measured by Lab 1 for the lake water unknowns was 1-2‰ different from
578 that measured by Lab 2, but again, no consistent offset emerged (Figure S4).
579   The SP values measured by the two laboratories showed larger standard deviations than
580 the $\delta^{15}N^{\alpha}$ and $\delta^{15}N^{\beta}$ individually, which is to be expected, since SP is a measure of difference
581 between the latter two parameters. The RMSD values, however, were all less than 3‰ for
582 atmosphere-equilibrated seawater, EMPA1, and EMPA3 (Table 3). This represents an
583 improvement on Mohn et al. (2014), who find an RMSD of 4.29‰ for SP measured by IRMS
584 laboratories. The Lake Lugano unknowns showed larger offsets than the reference materials
585 (Figure S4). The lake water sample from 10 m depth showed an especially large difference in SP
586 between Lab 1 and Lab 2: Lab 1 measured a mean SP of 16.43±1.35‰ at this depth, while Lab 2

measured a mean SP of 20.77±2.67‰ (Table 3). At 90 m depth, Lab 1 measured a mean SP of 54.40±1.23‰, and Lab 2 measured a mean SP of 55.09±1.69‰.

For $\delta^{18}O_{N2O}$, Lab 1 obtained consistently higher values than Lab 2, despite the application of a scale decompression, which should compensate for such offsets.[52] The only exception to this rule was the lake water unknown from 10 m depth, for which the $\delta^{18}O_{N2O}$ values measured by the two labs were statistically indistinguishable (Table 3; Figure S4). For the other samples and reference materials, the magnitude of this offset varied from 2.81‰ (EMPA3) to 6.80‰ (lake water unknown from 90 m). For reference materials EMPA1 and EMPA3, the $\delta^{18}O_{N2O}$ values measured by Lab 1 were 2-3‰ higher than the calibrated $\delta^{18}O_{N2O}$ (Tables 1 & 3), while the $\delta^{18}O_{N2O}$ values measured by Lab 2 did not exhibit such an offset. For atmosphere-equilibrated seawater, the $\delta^{18}O_{N2O}$ values measured by Lab 2 were ~3‰ lower than the calibrated $\delta^{18}O_{N2O}$ (Tables 1 & 3), while the $\delta^{18}O_{N2O}$ values measured by Lab 1 did not exhibit such an offset. This offset did not exhibit any dependence on N_2O concentration — rather, the variation in $\delta^{18}O_{N2O}$ values tended to be larger for lower peak areas, resulting in greater offsets, but without any measurable trend (cite figure or table?). Similarly, the linearity correction could not correct for the variation at lower peak areas, because this variation was random.

5. Conclusion: How to obtain high-quality N_2O isotopocule data using pyisotopomer

Using pyisotopomer and at least two reference materials (three characterized gases, assuming the N_2O reference tank is also calibrated), one can calculate scrambling for a given IRMS and apply those scrambling coefficients to calculate the isotopocule values of unknown samples. To ensure high-quality results from these calculations, we provide the following recommendations. Firstly, if scrambling has never been calculated for the IRMS or current filament, iterate through the scrambling calculation twice. Use the solution from the first iteration as the initial guess for subsequent calculations. This can be achieved with the "initialguess" argument to the Scrambling function of pyisotopomer. In a similar vein, use the default settings for the lower and upper bounds for both the Scrambling and Isotopomers solvers. These settings allow the solvers to search for solutions across the widest possible range of values. Secondly, to calculate scrambling, where possible, choose pairings of reference materials that bracket the range of unknowns but do not have $\delta^{15}N^{\alpha}$, $\delta^{15}N^{\beta}$, or $\delta^{18}O_{N2O}$ that lie far outside of this range. The same is true for scale decompression. Third, if the MATLAB version of pyisotopomer is used to calculate scrambling, the MATLAB version should also be used to calculate isotopocules. Finally, it is necessary to run paired reference materials daily to obtain accurate running estimates of γ and κ. It is recommended to calculate convert these daily estimates to a 1-week running average and use that average to calculate isotopocules. For a 1‰ precision in SP, the standard deviation of this running average should represent no more than a 0.2% uncertainty in γ and κ.

Using pyisotopomer in an intercalibration exercise and implementing the above recommendations, we find good agreement between the isotopocules measured by two different IRMS labs for both reference materials and natural lake samples. We conclude that while the intercalibration results demonstrate potential for further improvement in both precision and accuracy, the intercalibration of SP using a uniform scrambling calculation (pyisotopomer) presented here represents an improvement upon previous N_2O intercalibrations.

Data availability statement

References

1. Yung YL, Wang WC, Lacis AA. Greenhouse effect due to atmospheric nitrous oxide. *Geophys Res Lett*. 1976;3(10):619-621. doi:10.1029/GL003i010p00619

2. Smith C, Nicholls ZRJ, Armour K, et al. The Earth's Energy Budget, Climate Feedbacks, and Climate Sensitivity Supplementary Material. In: Masson-Delmotte V, Zhai P, Pirani A, et al., eds. *Climate Change 2021: The Physical Science Basis. Contribution of Working Group I to the Sixth Assessment Report of the Intergovernmental Panel on Climate Change*. Cambridge University Press; 2021. Accessed October 4, 2021. https://www.ipcc.ch/report/ar6/wg1/downloads/report/IPCC_AR6_WGI_Chapter_07_Supplementary_Material.pdf

3. Crutzen PJ. The influence of nitrogen oxides on the atmospheric ozone content. *Q J R Meteorol Soc*. 1970;96(408):320-325. doi:10.1002/qj.49709640815

4. Ravishankara AR, Daniel JS, Portmann RW. Nitrous Oxide (N2O): The Dominant Ozone-Depleting Substance Emitted in the 21st Century. *Science*. 2009;326(5949):123-125. doi:10.1126/science.1176985

5. Wuebbles DJ. Nitrous Oxide: No Laughing Matter. *Science*. 2009;326(5949):56-57. doi:10.1126/science.1179571

6. Müller R. The impact of the rise in atmospheric nitrous oxide on stratospheric ozone. *Ambio*. 2021;50(1):35-39. doi:10.1007/s13280-020-01428-3

7. Kim KR, Craig H. Nitrogen-15 and Oxygen-18 Characteristics of Nitrous Oxide: A Global Perspective. *Science*. 1993;262(5141):1855-1857. doi:10.1126/science.262.5141.1855

8. Pérez T, Trumbore SE, Tyler SC, Davidson EA, Keller M, Camargo PB de. Isotopic variability of N2O emissions from tropical forest soils. *Glob Biogeochem Cycles*. 2000;14(2):525-535. doi:10.1029/1999GB001181

9. Rahn T, Wahlen M. Stable Isotope Enrichment in Stratospheric Nitrous Oxide. *Science*. 1997;278(5344):1776-1778. doi:10.1126/science.278.5344.1776

10. Rahn T, Wahlen M. A reassessment of the global isotopic budget of atmospheric nitrous oxide. *Glob Biogeochem Cycles*. 2000;14(2):537-543. doi:10.1029/1999GB900070

11. Kim KR, Craig H. Two-isotope characterization of N20 in the Pacific Ocean and constraints on its origin in deep water. *Nature*. 1990;347(6288):58-61. doi:10.1038/347058a0

12. Dore JE, Popp BN, Karl DM, Sansone FJ. A large source of atmospheric nitrous oxide from subtropical North Pacific surface waters. *Nature*. 1998;396(6706):63-66. doi:10.1038/23921

675   13.   Naqvi SWA, Naik H, Jayakumar A, et al. Seasonal anoxia Over the Western Indian
676   Continental Shelf. In: Wiggert JD, Hood RR, Naqvi SWA, Brink KH, Smith SL, eds.
677   *Geophysical Monograph Series*. Vol 185. American Geophysical Union; 2009:333-345.
678   doi:10.1029/2008GM000745

679   14.   Yoshida N, Hattori A, Saino T, Matsuo S, Wada E. 15N/14N ratio of dissolved N2O in the
680   eastern tropical Pacific Ocean. *Nature*. Published online 1984. doi:10.1038/307442A0

681   15.   Yoshida N. 15N-depleted N2O as a product of nitrification. *Nature*. 1988;335(6190):528-
682   529. doi:10.1038/335528a0

683   16.   Barford CC, Montoya JP, Altabet MA, Mitchell R. Steady-State Nitrogen Isotope Effects of
684   N2 and N2O Production in Paracoccus denitrificans. *Appl Environ Microbiol*.
685   1999;65(3):989-994. doi:10.1128/AEM.65.3.989-994.1999

686   17.   Friedman L, Bigeleisen J. Oxygen and Nitrogen Isotope Effects in the Decomposition of
687   Ammonium Nitrate. *J Chem Phys*. 1950;18(10):1325-1331. doi:10.1063/1.1747471

688   18.   Toyoda S, Yoshida N. Determination of nitrogen isotopomers of nitrous oxide on a
689   modified isotope ratio mass spectrometer. *Anal Chem*. 1999;71(20):4711-4718.
690   doi:10.1021/ac9904563

691   19.   Brenninkmeijer C a. M, Röckmann T. Mass spectrometry of the intramolecular nitrogen
692   isotope distribution of environmental nitrous oxide using fragment-ion analysis. *Rapid
693   Commun Mass Spectrom*. 1999;13(20):2028-2033. doi:10.1002/(SICI)1097-
694   0231(19991030)13:20<2028::AID-RCM751>3.0.CO;2-J

695   20.   Röckmann T, Levin I. High-precision determination of the changing isotopic composition
696   of atmospheric N2O from 1990 to 2002. *J Geophys Res Atmospheres*. 2005;110(D21).
697   doi:10.1029/2005JD006066

698   21.   Yung YL, Miller CE. Isotopic Fractionation of Stratospheric Nitrous Oxide. *Science*.
699   1997;278(5344):1778-1780. doi:10.1126/science.278.5344.1778

700   22.   Yoshida null, Toyoda null. Constraining the atmospheric N2O budget from intramolecular
701   site preference in N2O isotopomers. *Nature*. 2000;405(6784):330-334.
702   doi:10.1038/35012558

703   23.   Röckmann T, Kaiser J, Brenninkmeijer CAM, et al. Isotopic enrichment of nitrous oxide
704   (15N14NO, 14N15NO, 14N14N18O) in the stratosphere and in the laboratory. *J Geophys
705   Res Atmospheres*. 2001;106(D10):10403-10410. doi:10.1029/2000JD900822

706   24.   Toyoda S, Yoshida N, Urabe T, et al. Temporal and latitudinal distributions of stratospheric
707   N2O isotopomers. *J Geophys Res Atmospheres*. 2004;109(D8). doi:10.1029/2003JD004316

708   25.   Kaiser J, Engel A, Borchers R, Rockmann T. Probing stratospheric transport and chemistry
709   with new balloon and aircraft observations of the meridional and vertical N2O isotope
710   distribution. *Atmos Chem Phys*. Published online 2006:22.

711 26. Park S, Atlas EL, Boering KA. Measurements of N2O isotopologues in the stratosphere:
712   Influence of transport on the apparent enrichment factors and the isotopologue fluxes to the
713   troposphere. *J Geophys Res Atmospheres*. 2004;109(D1). doi:10.1029/2003JD003731

714 27. Toyoda S, Yoshida N, Miwa T, et al. Production mechanism and global budget of N2O
715   inferred from its isotopomers in the western North Pacific. *Geophys Res Lett*. 2002;29(3):7-
716   1-7-4. doi:10.1029/2001GL014311

717 28. Sutka RL, Ostrom NE, Ostrom PH, Gandhi H, Breznak JA. Nitrogen isotopomer site
718   preference of N2O produced by Nitrosomonas europaea and Methylococcus capsulatus
719   Bath. *Rapid Commun Mass Spectrom RCM*. 2003;17(7):738-745. doi:10.1002/rcm.968

720 29. Sutka RL, Ostrom NE, Ostrom PH, et al. Distinguishing Nitrous Oxide Production from
721   Nitrification and Denitrification on the Basis of Isotopomer Abundances. *Appl Environ
722   Microbiol*. 2006;72(1):638-644. doi:10.1128/AEM.72.1.638-644.2006

723 30. Sutka RL, Ostrom NE, Ostrom PH, Gandhi H, Breznak JA. Nitrogen isotopomer site
724   preference of N2O produced by Nitrosomonas europaea and Methylococcus capsulatus
725   Bath. *Rapid Commun Mass Spectrom*. 2004;18(12):1411-1412. doi:10.1002/rcm.1482

726 31. Toyoda S, Mutobe H, Yamagishi H, Yoshida N, Tanji Y. Fractionation of N2O isotopomers
727   during production by denitrifier. *Soil Biol Biochem*. 2005;37(8):1535-1545.
728   doi:10.1016/j.soilbio.2005.01.009

729 32. Frame CH, Casciotti KL. Biogeochemical controls and isotopic signatures of nitrous oxide
730   production by a marine ammonia-oxidizing bacterium. *Biogeosciences*. 2010;7(9):2695-
731   2709. doi:https://doi.org/10.5194/bg-7-2695-2010

732 33. Schmidt HL, Werner RA, Yoshida N, Well R. Is the isotopic composition of nitrous oxide
733   an indicator for its origin from nitrification or denitrification? A theoretical approach from
734   referred data and microbiological and enzyme kinetic aspects. *Rapid Commun Mass
735   Spectrom*. 2004;18(18):2036-2040. doi:10.1002/rcm.1586

736 34. Ostrom NE, Pitt A, Sutka R, et al. Isotopologue effects during N2O reduction in soils and in
737   pure cultures of denitrifiers. *J Geophys Res Biogeosciences*. 2007;112(G2).
738   doi:10.1029/2006JG000287

739 35. Lewicka-Szczebak D, Augustin J, Giesemann A, Well R. Quantifying N2O reduction to N2
740   based on N2O isotopocules – validation with independent methods (helium incubation and
741   15N gas flux method). *Biogeosciences*. 2017;14(3):711-732. doi:https://doi.org/10.5194/bg-
742   14-711-2017

743 36. Casciotti KL, Forbes M, Vedamati J, Peters BD, Martin TS, Mordy CW. Nitrous oxide
744   cycling in the Eastern Tropical South Pacific as inferred from isotopic and isotopomeric
745   data. *Deep Sea Res Part II Top Stud Oceanogr*. 2018;156:155-167.
746   doi:10.1016/j.dsr2.2018.07.014

747 37. Kelly CL, Travis NM, Baya PA, Casciotti KL. Quantifying Nitrous Oxide Cycling Regimes
748   in the Eastern Tropical North Pacific Ocean With Isotopomer Analysis. *Glob Biogeochem*
749   *Cycles*. 2021;35(2):e2020GB006637. doi:https://doi.org/10.1029/2020GB006637

750 38. Pérez T, Trumbore SE, Tyler SC, et al. Identifying the agricultural imprint on the global
751   N2O budget using stable isotopes. *J Geophys Res Atmospheres*. 2001;106(D9):9869-9878.
752   doi:10.1029/2000JD900809

753 39. Yamulki S, Toyoda S, Yoshida N, Veldkamp E, Grant B, Bol R. Diurnal fluxes and the
754   isotopomer ratios of N2O in a temperate grassland following urine amendment. *Rapid*
755   *Commun Mass Spectrom*. 2001;15(15):1263-1269. doi:10.1002/rcm.352

756 40. Verhoeven E, Barthel M, Yu L, et al. Early season N$_2$O emissions under variable water
757   management in rice systems: source-partitioning emissions using isotope ratios along a
758   depth profile. *Biogeosciences*. 2019;16(2):383-408. doi:https://doi.org/10.5194/bg-16-383-
759   2019

760 41. Popp BN, Westley MB, Toyoda S, et al. Nitrogen and oxygen isotopomeric constraints on
761   the origins and sea-to-air flux of N2O in the oligotrophic subtropical North Pacific gyre.
762   *Glob Biogeochem Cycles*. 2002;16(4):12-1-12-10. doi:10.1029/2001GB001806

763 42. Yamagishi H, Westley MB, Popp BN, et al. Role of nitrification and denitrification on the
764   nitrous oxide cycle in the eastern tropical North Pacific and Gulf of California. *J Geophys*
765   *Res Biogeosciences*. 2007;112(G2). doi:10.1029/2006JG000227

766 43. Yamagishi H, Yoshida N, Toyoda S, Popp BN, Westley MB, Watanabe S. Contributions of
767   denitrification and mixing on the distribution of nitrous oxide in the North Pacific. *Geophys*
768   *Res Lett*. 2005;32(4). doi:10.1029/2004GL021458

769 44. Westley MB, Yamagishi H, Popp BN, Yoshida N. Nitrous oxide cycling in the Black Sea
770   inferred from stable isotope and isotopomer distributions. *Deep Sea Res Part II Top Stud*
771   *Oceanogr*. 2006;53(17-19):1802-1816. doi:10.1016/j.dsr2.2006.03.012

772 45. Farías L, Castro-González M, Cornejo M, et al. Denitrification and nitrous oxide cycling
773   within the upper oxycline of the eastern tropical South Pacific oxygen minimum zone.
774   *Limnol Oceanogr*. 2009;54(1):132-144. doi:10.4319/lo.2009.54.1.0132

775 46. Bourbonnais A, Letscher RT, Bange HW, et al. N2O production and consumption from
776   stable isotopic and concentration data in the Peruvian coastal upwelling system. *Glob*
777   *Biogeochem Cycles*. 2017;31(4):678-698. doi:10.1002/2016GB005567

778 47. Toyoda S, Yoshida O, Yamagishi H, Fujii A, Yoshida N, Watanabe S. Identifying the
779   origin of nitrous oxide dissolved in deep ocean by concentration and isotopocule analyses.
780   *Sci Rep*. 2019;9(1):1-9. doi:10.1038/s41598-019-44224-0

781 48. Toyoda S, Kakimoto T, Kudo K, et al. Distribution and Production Mechanisms of N2O in
782   the Western Arctic Ocean. *Glob Biogeochem Cycles*. 2021;35(4):e2020GB006881.
783   doi:https://doi.org/10.1029/2020GB006881

784   49.   Kaiser J, Park S, Boering KA, Brenninkmeijer CAM, Hilkert A, Röckmann T. Mass
785   spectrometric method for the absolute calibration of the intramolecular nitrogen isotope
786   distribution in nitrous oxide. *Anal Bioanal Chem*. 2004;378(2):256-269.
787   doi:10.1007/s00216-003-2233-2

788   50.   Westley MB, Popp BN, Rust TM. The calibration of the intramolecular nitrogen isotope
789   distribution in nitrous oxide measured by isotope ratio mass spectrometry. *Rapid Commun*
790   *Mass Spectrom*. 2007;21(3):391-405. doi:10.1002/rcm.2828

791   51.   Ostrom NE, Gandhi H, Coplen TB, et al. Preliminary assessment of stable nitrogen and
792   oxygen isotopic composition of USGS51 and USGS52 nitrous oxide reference gases and
793   perspectives on calibration needs. *Rapid Commun Mass Spectrom*. 2018;32(15):1207-1214.
794   doi:10.1002/rcm.8157

795   52.   Mohn J, Wolf B, Toyoda S, et al. Interlaboratory assessment of nitrous oxide isotopomer
796   analysis by isotope ratio mass spectrometry and laser spectroscopy: current status and
797   perspectives. *Rapid Commun Mass Spectrom*. 2014;28(18):1995-2007.
798   doi:10.1002/rcm.6982

799   53.   Kaiser J, Röckmann T, Brenninkmeijer CAM. Complete and accurate mass spectrometric
800   isotope analysis of tropospheric nitrous oxide. *J Geophys Res Atmospheres*.
801   2003;108(D15). doi:10.1029/2003JD003613

802   54.   Wankel SD, Ziebis W, Buchwald C, et al. Evidence for fungal and chemodenitrification
803   based N 2 O flux from nitrogen impacted coastal sediments. *Nat Commun*. 2017;8(1):1-11.
804   doi:10.1038/ncomms15595

805   55.   Baertschi P. Absolute18O content of standard mean ocean water. *Earth Planet Sci Lett*.
806   1976;31(3):341-344. doi:10.1016/0012-821X(76)90115-1

807   56.   Jabeen I, Kusakabe M. Determination of δ 17O values of reference water samples VSMOW
808   and SLAP. *Chem Geol*. 1997;143:115-119. doi:10.1016/S0009-2541(97)00109-5

809   57.   Magyar PM, Orphan VJ, Eiler JM. Measurement of rare isotopologues of nitrous oxide by
810   high-resolution multi-collector mass spectrometry. *Rapid Commun Mass Spectrom*.
811   2016;30(17):1923-1940. doi:10.1002/rcm.7671

812   58.   Kelly CL. *Ckelly314/Pyisotopomer: Version 0.0.1*. Zenodo; 2021.
813   doi:10.5281/zenodo.5031218

814   59.   McIlvin MR, Casciotti KL. Technical updates to the bacterial method for nitrate isotopic
815   analyses. *Anal Chem*. 2011;83(5):1850-1856. doi:10.1021/ac1028984

816   60.   McIlvin MR, Casciotti KL. Fully automated system for stable isotopic analyses of dissolved
817   nitrous oxide at natural abundance levels. *Limnol Oceanogr Methods*. 2010;8(2):54-66.
818   doi:10.4319/lom.2010.8.54

819   61.   Dutton GS, Elkins JW, Hall BD. Nitrous Oxide data from the NOAA/ESRL halocarbons in
820   situ program. Published online 2021. Accessed November 19, 2021.
821   https://data.nodc.noaa.gov/cgi-bin/iso?id=gov.noaa.ncdc:C01556

822   62.   Santoro AE, Buchwald C, McIlvin MR, Casciotti KL. Isotopic Signature of N2O Produced
823   by Marine Ammonia-Oxidizing Archaea. *Science*. 2011;333(6047):1282-1285.
824   doi:10.1126/science.1208239

825   63.   Cohen J. *Statistical Power Analysis for the Behavioral Sciences*. Academic Press; 2013.

826   64.   Lorquet JC, Cadet C. Excited states of gaseous ions: I. Selection rules in photoelectron
827   spectroscopy and photoionization. The case of N2O+. *Int J Mass Spectrom Ion Phys*.
828   1971;7(3):245-254. doi:10.1016/0020-7381(71)80020-7

829   65.   Märk E, Märk TD, Kim YB, Stephan K. Absolute electron impact ionization cross section
830   from threshold up to 180 eV for N2O+e→N2O++2e and the metastable and collision
831   induced dissociation of N2O+. *J Chem Phys*. 1981;75(9):4446-4453. doi:10.1063/1.442611

832   66.   Bigeleis J. Isotope chemistry has opened new areas of chemic,al physics, geochemistry, and
833   molecular biologry. Published online 1965:10.

834   67.   Begun GM, Landau L. Metastable Transitions in N2O+. *J Chem Phys*. 1962;36(4):1083-
835   1084. doi:10.1063/1.1732641

836
837

838 **Table 1:** Reference materials for N_2O isotopic analysis and intercalibration. The laboratories
839 participating in the intercalibration exercise were at Stanford University ("Lab 1") and the
840 University of Basel ("Lab 2").
841

Reference material	$\delta^{15}N^{\alpha}$	$\delta^{15}N^{\beta}$	SP	$\delta^{15}N^{bulk}$	$\delta^{18}O_{N2O}$	Calibration by
	(‰ vs. air N₂)				(‰ vs. VSMOW)	
S2 reference gas	5.55	-12.87	18.42	-3.66	32.73	S. Toyoda, Tokyo Tech
B6 reference gas	-0.40	-0.15	-0.26	-0.28	41.95	Lab 1 internal standard
Atmosphere-equilibrated seawater	15.70	-3.30	19.00	6.20	44.30	Mohn et al. (2014)
EMPA1 reference gas (CA06261)	-22.21	-49.28	27.07	-35.75	26.94	J. Mohn, EMPA
EMPA2 reference gas (CA08214)	1.71	94.44	-92.73	48.08	36.01	J. Mohn, EMPA
EMPA3 reference gas (53504)	17.11	-3.43	20.54	6.84	35.39	J. Mohn, EMPA
	^{31}R	^{45}R	^{46}R			
Lab 1 pure N_2O direct injection	0.003733763	0.007741025	0.002101295			S. Toyoda, Tokyo Tech
Lab 2 pure N_2O direct injection	0.004049069	0.007738762	0.002100262			J. Mohn, EMPA

842
843
844

845 **Table 2:** Performance tests of pyisotopomer. A) The initial guess x0 used to solve for γ and κ
846 was varied from γ=κ=0.05 to γ=κ=0.20. B) The lower bounds used to solve for γ and κ were
847 varied from γ=κ=0.0 to γ=κ=0.08. C) The upper bounds used to solve for γ and κ was varied
848 from γ=κ=0.4 to γ=κ=1.0. D) The γ and κ used to calculated ^{31}R for the direct reference injection
849 were varied. For each test, the resulting range of solutions for γ and κ were used to calculate
850 isotopocule values for test reference materials. Reported values are the means and standard
851 deviations of the range of 50 solutions.
852

Sample ID	$\delta^{15}N^{\alpha}$	$\delta^{15}N^{\beta}$	SP	$\delta^{15}N^{bulk}$	$\delta^{18}O_{N2O}$
			(‰ vs. air N₂)		*(‰ vs. VSMOW)*
A. Varying initial guess x0					
Atmosphere-equilibrated seawater #1	15.45±0.02	-3.59±0.02	19.03±0.03	5.93±0.00	45.39±0.00
Atmosphere-equilibrated seawater #2	14.85±0.04	-3.22±0.04	18.07±0.08	5.82±0.00	46.45±0.00
S2 reference gas #1	5.18±0.07	-12.28±0.07	17.46±0.13	-3.55±0.00	33.30±0.00
S2 reference gas #2	5.19±0.05	-12.52±0.05	17.71±0.10	-3.66±0.00	34.31±0.00
B. Varying lower bounds					
Atmosphere-equilibrated seawater #1	15.51±0.00	-3.66±0.00	19.17±0.00	5.93±0.00	45.39±0.00
Atmosphere-equilibrated seawater #2	14.97±0.00	-3.34±0.00	18.30±0.00	5.82±0.00	46.45±0.00
S2 reference gas #1	5.32±0.00	-12.42±0.00	17.74±0.00	-3.55±0.00	33.30±0.00
S2 reference gas #2	5.32±0.00	-12.64±0.00	17.96±0.00	-3.66±0.00	34.31±0.00
C. Varying upper bounds					
Atmosphere-equilibrated seawater #1	15.51±0.00	-3.65±0.00	19.16±0.01	5.93±0.00	45.39±0.00
Atmosphere-equilibrated seawater #2	14.97±0.00	-3.33±0.00	18.30±0.00	5.82±0.00	46.45±0.00
S2 reference gas #1	5.31±0.00	-12.42±0.00	17.73±0.00	-3.55±0.00	33.30±0.00
S2 reference gas #2	5.32±0.00	-12.64±0.00	17.96±0.00	-3.66±0.00	34.31±0.00
D. Varying ref. injection scrambling					
Atmosphere-equilibrated seawater #1	15.40±0.13	-3.54±0.13	18.94±0.27	5.93±0.00	45.39±0.00
S2 reference gas #1	5.20±0.13	-12.30±0.13	17.50±0.27	-3.55±0.00	33.30±0.00

853
854
855

Table 3: N_2O isotopic composition of four reference materials and two unknowns analyzed by two IRMS laboratories. $\delta^{15}N^\alpha$, $\delta^{15}N^\beta$, SP, and $\delta^{15}N^{bulk}$ are reported in ‰ vs. Air N_2, and $\delta^{18}O_{N2O}$ is reported in ‰ vs. VSMOW. Uncertainties are standard deviations of replicate bottles and do not include the propagation of calibration uncertainties. The root-mean square deviation (RMSD) was calculated with respect to the calibration data presented in Table 1.

| Reference gas		$\delta^{15}N^\alpha$	$\delta^{15}N^\beta$	SP	$\delta^{15}N^{bulk}$	$\delta^{18}O_{N2O}$
		(‰ vs. air N₂)				*(‰ vs. VSMOW)*
Atmosphere-equilibrated seawater	mean (Lab 1)	15.46±0.72	-3.12±2.00	18.58±2.43	6.17±0.89	44.67±2.08
	mean (Lab 2)	16.88±1.82	-4.21±1.75	21.09±3.51	6.34±0.33	40.81±1.04
	RMSD (Labs 1 & 2)	1.20	1.81	2.73	0.71	6.49
EMPA1	mean (Lab 1)	-17.77±1.69	-43.88±1.89	26.12±3.55	-30.83±0.23	30.31±1.27
	mean (Lab 2)	-22.41±1.55	-49.19±2.42	26.78±3.71	-35.80±0.83	27.01±1.68
	RMSD (Labs 1 & 2)	2.57	3.10	2.89	2.46	2.04
EMPA2*	mean (Lab 1)	2.49±1.33	82.89±1.69	-80.40±2.39	42.69±0.94	39.36±0.79
	mean (Lab 2)	-10.43±1.44	102.16±3.86	-112.60±4.46	45.87±1.88	35.44±1.35
	RMSD (Labs 1 & 2)	10.96	9.82	19.53	3.59	2.07
EMPA3	mean (Lab 1)	16.55±1.75	-2.90±0.95	19.99±2.49	7.10±0.66	37.85±1.25
	mean (Lab 2)	17.11±1.31	-3.51±1.30	20.62±2.28	6.80±0.64	35.04±3.34
	RMSD (Labs 1 & 2)	1.31	1.04	2.13	0.50	2.32
Unknown #1 (Lake Lugano, 10m depth)	mean (Lab 1)	11.93±0.29	-4.51±1.05	16.43±1.35	3.71±0.38	44.56±1.16
	mean (Lab 2)	14.49±1.34	-6.28±1.47	20.77±2.67	4.10±0.44	44.90±1.64
Unknown #2 (Lake Lugano, 90m depth)	mean (Lab 1)	22.20±0.55	-32.20±0.68	54.40±1.23	-5.00±0.08	60.68±0.04
	mean (Lab 2)	21.26±1.91	-33.81±0.22	55.09±1.69	-6.26±1.06	53.88±4.69
*Large errors are due to exclusion from scrambling calibration						
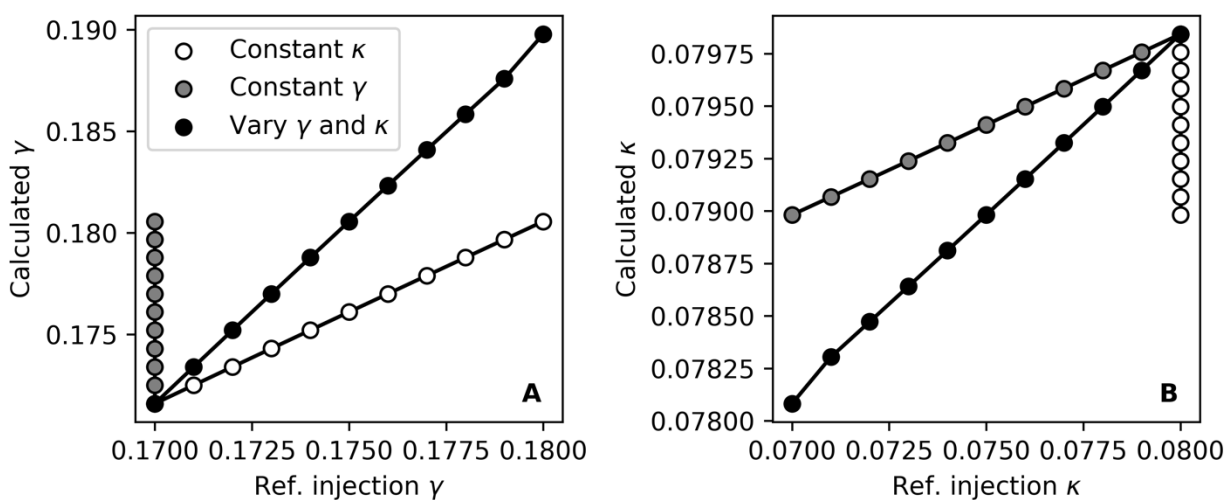
Figure 1. Solutions for γ (A) and κ (B) calculated across a range of theoretical γ and κ for the direct reference injection: changing the reference injection γ and holding the reference injection κ constant (white), changing the reference injection κ and holding the reference injection γ constant (gray), changing both reference injection γ and κ (black).

pyisotoper 26

869
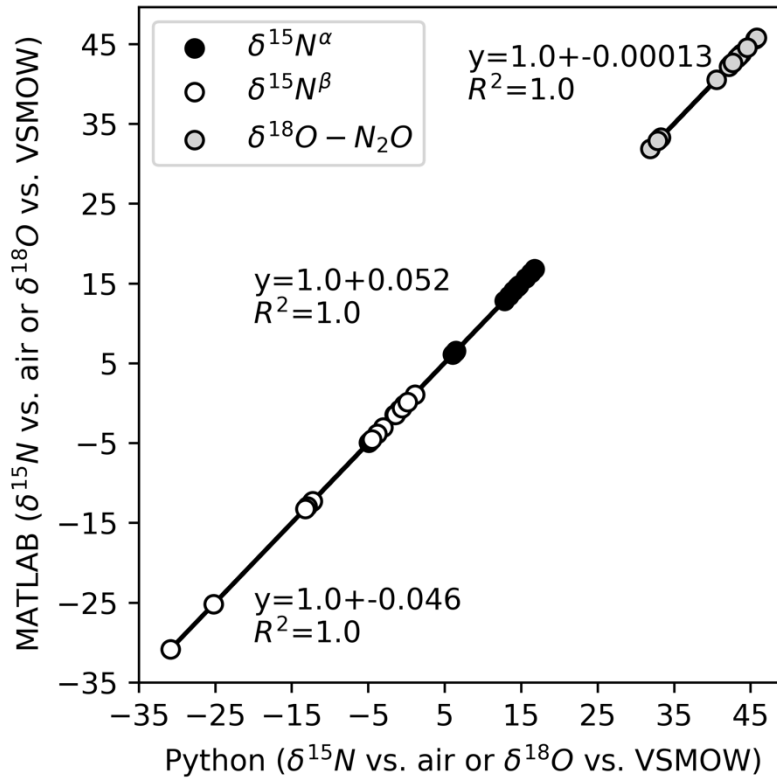
Figure 2. Comparison of isotopocule results for Python and MATLAB versions of pyisotopomer.

871

872

873
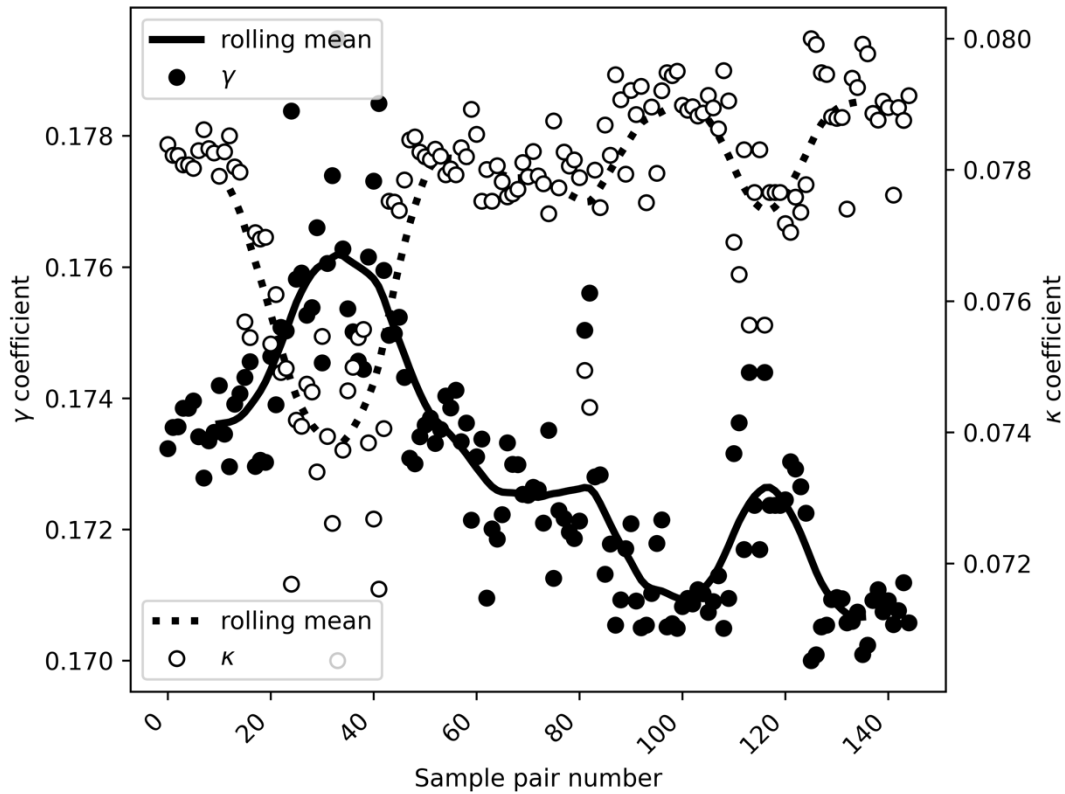
**Figure 3.** Scrambling coefficients for the Lab 1 IRMS from October 2018 to January 2021.
Individual pairs of scrambling coefficients, calculated from individual pairs of reference
materials, are shown as a scatter plot. A rolling mean with a 20-value window (roughly
equivalent to one week of analysis) is plotted for each coefficient. The x-axis is sample pair
number, rather than date, to better visualize short-term variability.

879

880
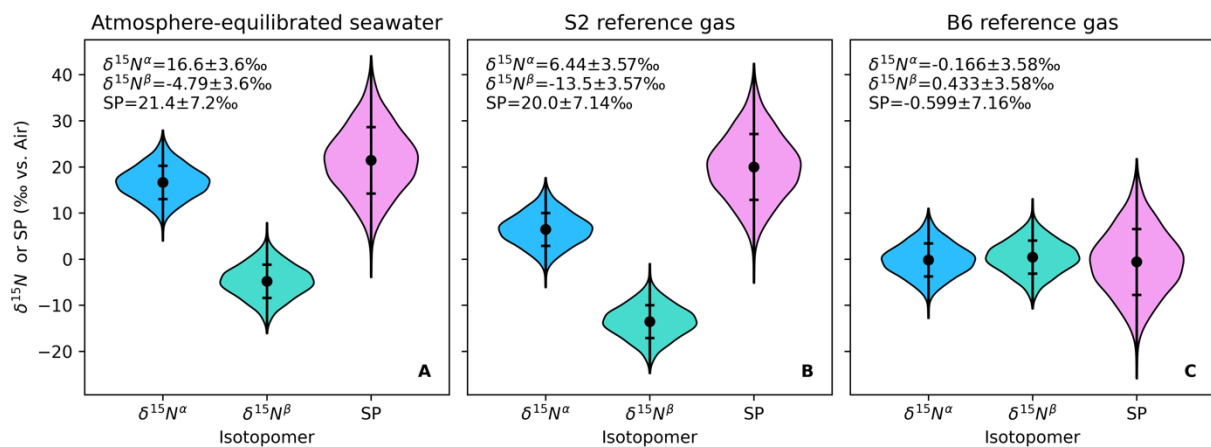
Figure 4: Isotopocule values and error associated with an uncertainty of ±0.00192 in γ and
±0.00184 in κ, based on Monte Carlo simulation results. The violin plots are based on a kernel

883   density estimate of the distribution and the values plotted and reported on each figure show the
884   mean value $\pm 1\sigma$.
885

Supplementary material

pyisotopomer: A Python package for obtaining nitrous oxide isotopocules from isotope ratio mass spectrometry

Colette L. Kelly,[1*] Cara Manning,[2] Claudia Frey,[3] Noah Gluschankoff,[1] and Karen L. Casciotti

1. Stanford University, Department of Earth System Science, Stanford, CA 94305, USA

2. University of Connecticut, Department of Marine Sciences, Groton, CT 06340, USA

3. Department of Environmental Science, University of Basel, Basel, Switzerland.

* Correspondence to: Colette L. Kelly (clkelly@stanford.edu).

Table S1: Different pairings of reference materials. Pooled standard deviations of γ and κ calculated from different pairings of reference materials, and the corresponding pooled standard deviations of $\delta^{15}N^{\alpha}$, $\delta^{15}N^{\beta}$, and SP, are shown for tests performed on the Lab 1 and Lab 2 IRMS. Pooled standard deviations are also shown for scrambling and isotopomer calculations done in the MATLAB and Python versions of the software.

|			Pooled standard deviations		
Test	γ	κ	$\delta^{15}N^{\alpha}$	$\delta^{15}N^{\beta}$	SP
	(% uncertainty*)	(% uncertainty*)	(‰ $vs.AirN_2$)	(‰ $vs.AirN_2$)	(‰ $vs.AirN_2$)
Lab 1 three ref. pairings, no extreme values	0.39	0.16	0.47	0.44	0.91
Lab 2 three ref. pairings, incl. extreme values	0.77	1.17	2.54	2.29	4.83
Lab 2 one ref. pairing, excl. extreme values	0.15	0.61	(see section 4.7 for precision between replicates)		
MATLAB vs. Python	0.44	0.93	0.028	0.026	0.054
*Percent uncertainties represent pooled SD as a percentage of the mean					
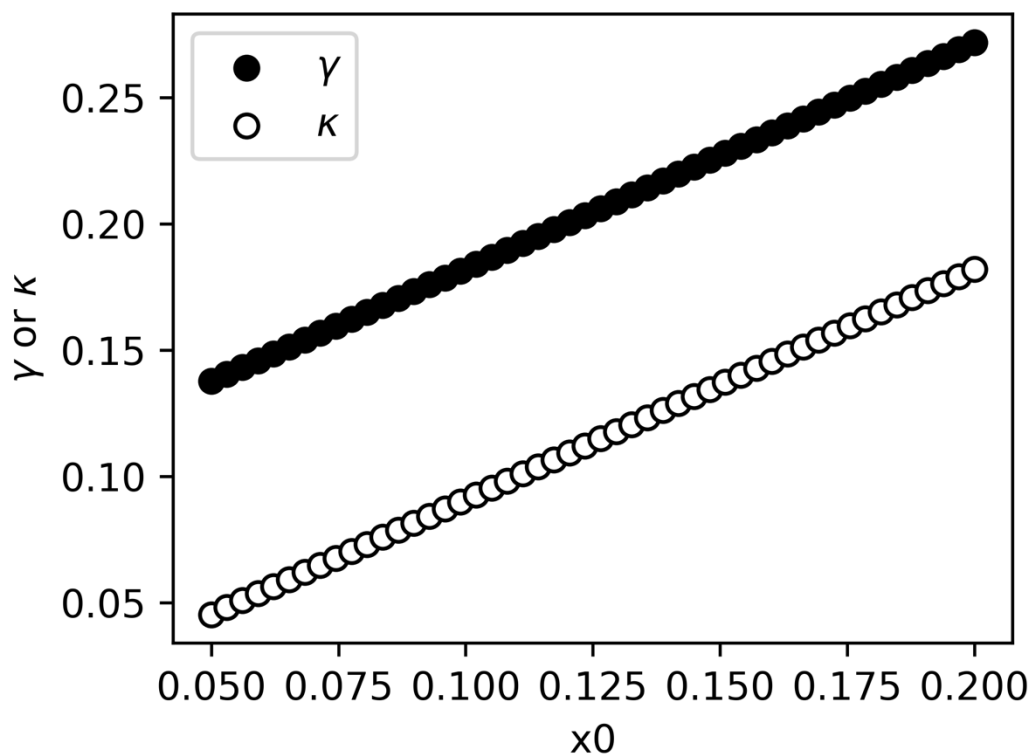
Figure S1. Solutions for γ and κ calculated across a range of initial guesses (x0) for the least squares solver function at the core of pyisotopomer. The default values for x0 are γ=0.17 and κ=0.08, based on the performance of the ThermoFinnigan Delta V mass spectrometer at Lab 1.
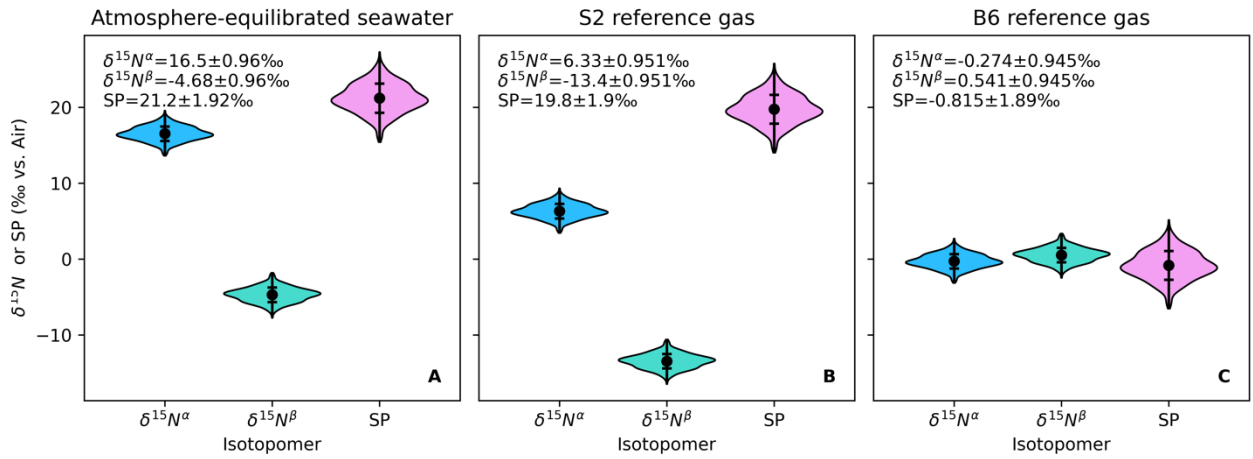
Figure S2: Isotopocule values and error associated with an uncertainty of $\pm 6.83 \times 10^{-4}$ in γ and $\pm 1.48 \times 10^{-4}$ in κ, based on Monte Carlo simulation results. The violin plots are based on a kernel density estimate of the distribution and show the mean value $\pm 1\sigma$.
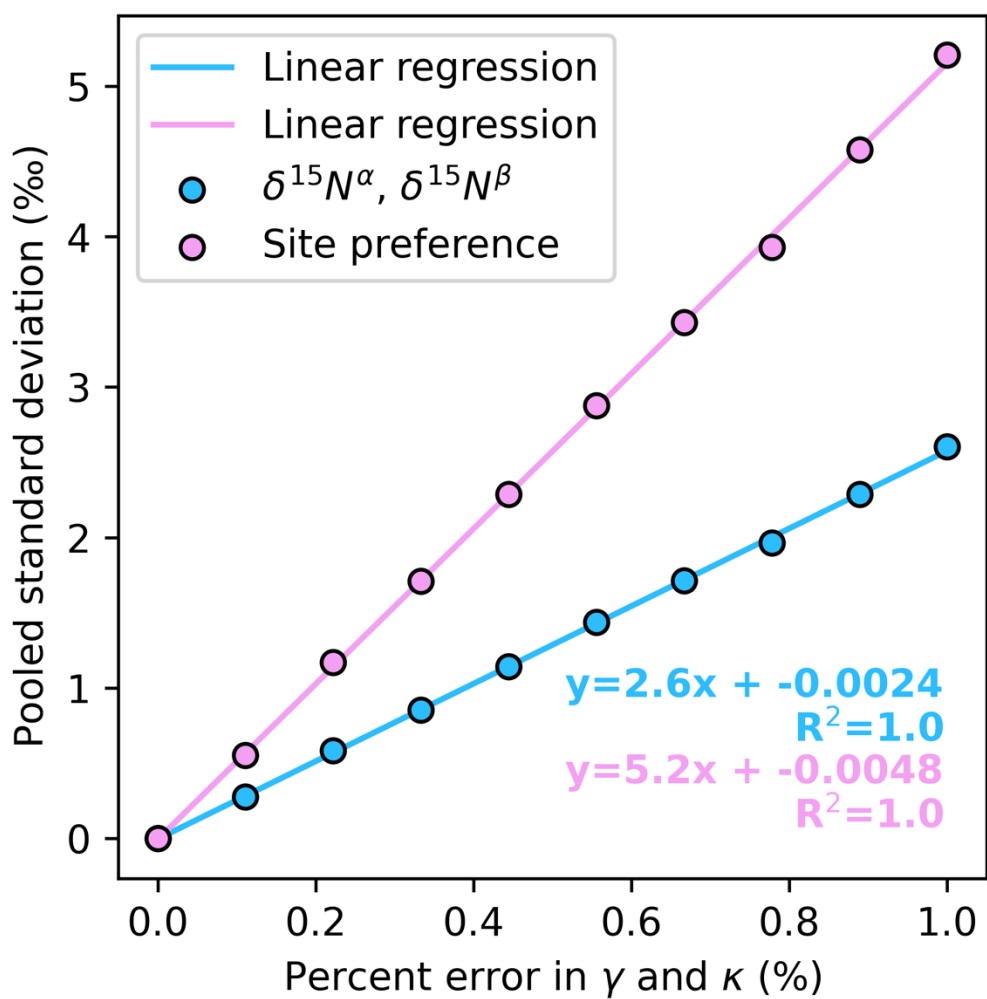
Figure S3: Pooled standard deviation of $\delta^{15}N^\alpha$, $\delta^{15}N^\beta$, and SP resulting from increasing relative uncertainties in γ and κ. Each point corresponds to 1,000 values of γ and κ sampled from a distribution with standard deviation equal to the given level of uncertainty, and the corresponding pooled standard deviation of 1,000 simulated values of $\delta^{15}N^\alpha$, $\delta^{15}N^\beta$, and SP.
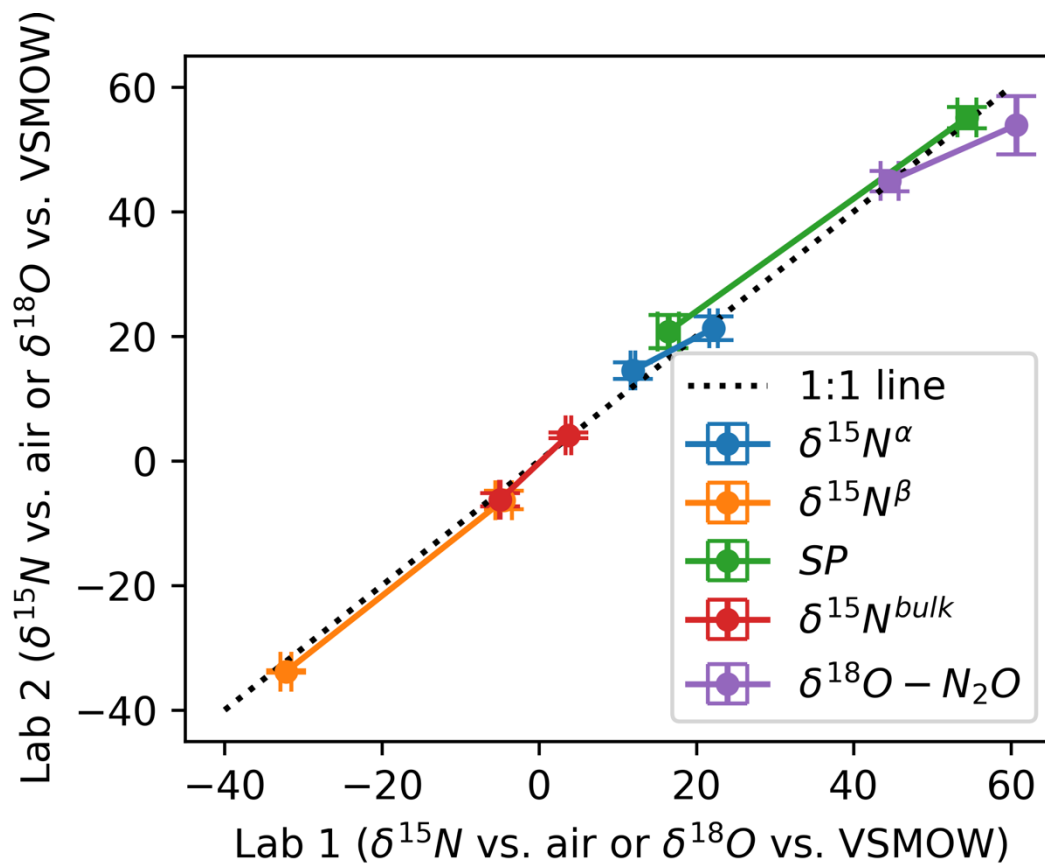
Figure S4: Intercalibration results for lake water unknowns taken at 10 meters and 90 meters depth from lake Lugano in Switzerland. Independent measurements of the isotopic composition of N_2O in each sample, performed by Lab 1 and Lab 2, respectively, are plotted against each other. Data points represent the mean from replicate bottles taken at the same depth (n=2-5) and error bars represent one standard deviation. A one-to-one line (black dashed line) is plotted for comparison.